Healed injuries to *Canis chihliensis* from early Pleistocene Nihewan beds, China, suggest family care for ancestral wolves

Hao-Wen Tong[1,2,*], Xi Chen[3], Bei Zhang[1,2,4], Bruce Rothschild[5], Stuart C. White[6], Mairin Balisi[7], and Xiaoming Wang[1,7,*]

[1] Key Laboratory of Vertebrate Evolution and Human Origins of Chinese Academy of Sciences, Institute of Vertebrate Paleontology and Paleoanthropology, Chinese Academy of Sciences, Beijing, China
[2] CAS Center for Excellence in Life and Paleoenvironment, Beijing, China
[3] Nanjing Normal University, Nanjing, China
[4] University of Chinese Academy of Sciences, Beijing, China
[5] Department of Vertebrate Paleontology, Carnegie Museum of Natural History, Pittsburgh, Pennsylvania, USA
[6] School of Dentistry, University of California, Los Angeles, California, USA
[7] Natural History Museum of Los Angeles County, California, USA.

Corresponding Authors:
Xiaoming Wang
900 Expedition Blvd, Los Angeles, California, 90007, USA
Email address: xwang@nhm.org
Haowen Tong
142 Xizhimenwai Dajie, Western District, Beijing 100044, China
Email address: tonghaowen@ivpp.ac.cn

Abstract

Collaborative hunting by complex social groups is a hallmark of large dogs (Mammalia: Carnivora: Canidae), whose teeth also tend to be hypercarnivorous, showing a specialization toward increased cutting edges for meat consumption and robust p4-m1 complex for cracking bone. The deep history of canid pack hunting is obscure, however, because behavioral evidence is rarely preserved in fossils. Dated to the early Pleistocene (~1.2 Ma), *Canis chihliensis* from the Nihewan Basin of northern China is one of the earliest canines to feature a large body size and hypercarnivorous dentition. We present the first known record of dental infection in *C. chihliensis*, likely inflicted by processing hard food, such as bone. An individual also suffered a displaced fracture of its tibia and, despite such an incapacitating injury, survived the trauma to

37   heal. The long period required for healing the compound fracture implicates social hunting and
38   family care (food-sharing). Comparison with abundant paleopathological records of the
39   putatively pack-hunting late Pleistocene dire wolf, *Canis dirus*, at the Rancho La Brea asphalt
40   seeps in southern California, U.S.A., suggests similarity in feeding behavior and sociality
41   between Chinese and American *Canis* across space and time. Pack hunting in *Canis* can thus be
42   traced back to the early Pleistocene, well before the appearance of modern wolves.
43

44   Introduction

45   Large, hypercarnivorous dogs (family Canidae)—such as gray wolves (*Canis lupus*), African
46   hunting dogs (*Lycaon pictus*), and Asian dholes (*Cuon alpinus*)—are known to be highly social
47   because of their need for collaborative hunting (Van Valkenburgh 1991). In all three species,
48   energetic requirements necessitate that they pursue prey species that are larger than themselves
49   (Carbone et al. 1999). But, unlike their felid (cat family) counterparts, canids lack retractile
50   claws and are usually unable to bring down their prey single-handedly (Wang et al. 2008),
51   making collaborative (pack) hunting a useful compensatory strategy. Despite the importance of
52   pack hunting as a key biological indicator for social interactions, trophic relationship, and diets,
53   however, fossil records rarely preserve direct information on behavior.
54   Discovery of an injured and healed skeleton and jaws of a large ancestral wolf, *Canis*
55   *chihliensis*, from the early Pleistocene hominine site of Nihewan Basin, northern China, is of
56   considerable interest in inferring their social behavior. Evidence of healing raises the possibility
57   that individuals survived incapacitating injuries by sharing food with family members (Palmqvist
58   et al. 1999), a question to be explored in this paper.
59

60   Materials & Methods

61   The methods employed in this study include morphological observations, CT scanning, and X-
62   ray examination. CT slicing intervals followed that of Rothschild et al. (1994). The osteological
63   terms are from Mescher (2018). The stages of fracture healing follow Edge-Hughes & Nicholson
64   (2007). Age determination follows Sumner-Smith (1966) for epiphyseal fusion and Gipson et al.
65   (2000) for tooth wear. Body-mass estimates were calculated using regressions on canid femur
66   shaft diameter by Anyonge & Roman (2006) and m1 length by Van Valkenburgh (1990).
67   Permission for excavation was granted by the State Administration of Cultural Heritage with a
68   permit number of 2018-090.
69

70   **Institution and Locality Abbreviations. HPICR**, Hebei Province Institute of Cultural Relics;
71   **IVPP**, Institute of Vertebrate Paleontology and Paleoanthropology; **MNHN**,
72   Muséum national d'Histoire naturelle; **NM**, Nihewan Museum; **NNNRM**, Nihewan National

73 Nature Reserve Management; **SSMZ**, Shanshenmiaozui; **TNHM**, Tianjin Natural History
74 Museum; **V,** Prefix in the catalog numbers for vertebrate fossils in IVPP.
75 **Morphological Abbreviations: DAP:** anteroposterior diameter; **DT:** transverse diameter; **MC:**
76 medullar cavity; **NF:** nutrient foramen.
77
78 **Locality and Fauna**. A large sample of early Pleistocene wolf, *Canis chihliensis*, comprising
79 more than 200 specimens including excellently preserved pathological conditions, affords an
80 opportunity to examine the social consequences of family care for the disabled. A left dentary
81 (IVPP V17755.11), a right dentary (IVPP V17755.12), and a right tibia (IVPP V18139.20) of
82 *Canis chihliensis* are all from the Shanshenmiaozui (SSMZ) Site in Nihewan Basin. *C.*
83 *chihliensis* from SSMZ is dominated by older individuals as inferred from wear on teeth (Chen
84 2018; Chen & Tong 2015). The SSMZ locality (40°13' 08"N, 114° 39' 54"E) lies at the southern
85 bank of the Sangganhe River, and at the edge of the Haojiatai fluviolacustrine platform in
86 Yangyuan County, Hebei Province (Fig. S1). The fossiliferous layer was dated to ca. 1.2 Ma by
87 magnetostratigraphy and associated fauna (Liu et al. 2016; Tong et al. 2011).
88 Canids are the most abundant carnivorans in the Early Pleistocene Nihewan Fauna (Qiu
89 2000; Teilhard de Chardin & Piveteau 1930), as also confirmed by our recent excavations at
90 SSMZ (Fig. S2). The dominate taxon of the canid guild in the SSMZ Fauna is *Canis chihliensis*
91 (Tong et al. 2011; Tong et al. 2012). The mammalian fauna associated with *C. chihliensis* at the
92 SSMZ site are as follows: *Lepus* sp., *Ochotona* sp., Pantherinae gen. et sp. indet., *Pachycrocuta*
93 sp., *Mammuthus trogontherii*, *Coelodonta nihowanensis*, *Elasmotherium peii*, *Proboscidipparion*
94 sp., *Equus sanmeniensis*, *Sus* sp., *Eucladoceros boulei*, *Spirocerus wongi*, *Bison palaeosinensis*,
95 and *Gazella sinensis*. Our fieldwork between 2015-2018 recovered additional taxa, e.g. *Alactaga*
96 sp. (represented by metacarpal), *Acinonyx* sp. (radius), *Panthera* sp. (partial mandible and manus
97 bones), *Lynx* sp. (partial mandible with m1, mandible), *Paracamelus* sp. (partial metatarsal),
98 *Pseudodama* sp. (partial antler and metacarpal), and *Gazella subgutturosa* (metatarsal) (Tong &
99 Chen 2015; Tong et al. 2017; Tong et al. 2018; Tong et al. 2011; Tong et al. 2012; Tong & Wang
100 2014; Tong & Zhang 2019).
101
102 **Rancho La Brea *Canis dirus*.** The best records of paleopathology in extinct canids are from the
103 world's largest collection of late Pleistocene dire wolf, *Canis dirus*, from the Rancho La Brea
104 asphalt seeps in Los Angeles, California, U.S.A. The Rancho La Brea paleopathology collection
105 comprises about 3,200 specimens of dire wolves assembled from over 200,000 specimens
106 representing a minimum of 3,500 individuals (dire wolves represent greater than 50% of all
107 mammal specimens from the Rancho La Brea) (Shaw & Ware 2018). As the largest *Canis* that
108 ever lived and presumably preferring larger prey, dire wolves are widely considered a social
109 predator (Anyonge & Roman 2006; Carbone et al. 2009; Hemmer 1978; Merriam 1912; Stock
110 1930; Van Valkenburgh & Hertel 1998; Van Valkenburgh & Sacco 2002). The Rancho La Brea
111 dire wolf collection preserves a range of pathological conditions throughout the skeleton
112 (Hartstone-Rose et al. 2015; Lawler et al. 2017; Moodie 1918; Shaw & Howard 2015; Stock

113 1930; Ware 2005), with particularly debilitating examples offering evidence that strong social
114 bonds existed to allow weakened or disabled individuals to survive for extended periods of time
115 (Shaw & Howard 2015; Shaw & Ware 2018).
116 Focusing on *Canis dirus* from a single deposit (Pit 61/67) at Rancho La Brea, Brown et al.
117 (2017) quantified patterns of traumatic pathology—injuries that likely resulted from hunting,
118 including healed fractures and evidence of severe or chronic muscle strain as well as
119 osteoarthritis—and predicted skull injuries to be common because of the probability of being
120 kicked while chasing prey. Contrary to expectation, the cranium showed a low incidence of
121 traumatic injury (1.6%) and the dentary even less so (0.18%) (Brown et al. 2017). This study,
122 however, excluded dental injuries likely incurred from feeding—such as abscesses and alveolar
123 resorption stemming from infection—which were also sustained by and preserved in *C. dirus*
124 from Rancho La Brea. In the current study, we quantify these dental injuries, as well as traumatic
125 damage to the dire wolf tibia, for comparison with dental and tibial injuries in *C. chihliensis*.

126 ## Results

127 **Taxonomic and Phylogenetic Remarks**. As far as we are aware, there are few reports of
128 debilitating injuries to large hypercarnivorous canines in the fossil record, including early
129 Pleistocene *Canis falconeri* from Venta Micena of Spain (Palmqvist et al. 1999), *Cuon* from late
130 Pleistocene of Italy (Iurino & Sardella 2014), and the latest Pleistocene occurrences of *Canis*
131 *dirus* in the Rancho La Brea asphalt seeps (Shaw & Howard 2015). This is despite a generally
132 excellent fossil record for large canids in the late Cenozoic because of canids' preference for
133 mid-latitude open habitats, where terrestrial fossil records are best preserved and most
134 extensively explored (Tedford et al. 2009; Wang 1994; Wang et al. 2008; Wang et al. 1999).
135 The holotype of *Canis chihliensis* was originally described based on a maxillary fragment
136 with P3-M2 from Feng-Wo at Huang-Lu village (Locality 64) in Huailai County, Hebei (Chihli)
137 Province by Zdansky (1924). Teilhard de Chardin & Piveteau (1930) referred additional
138 specimens to this species from Nihewan Basin. Rook (1994) synonymized *C. chihliensis* with *C.*
139 *antonii* Zdansky, 1924, but Tedford et al. (2009) returned to *C. chihliensis* by restricting the
140 concept to large Nihewan *Canis*. The systematics of *C. chihliensis* from SSMZ has been treated
141 by Tong et al. (2012)
142 Rook (1994) and Sotnikova (2001) referred the Pliocene-Early Pleistocene species *Canis*
143 *falconeri* from Europe, *C. antonii* from Asia and *C. africanus* from Africa to the supraspecific
144 group *Canis* (*Xenocyon*) ex gr. *falconeri*. All of them readily fall into the category of
145 hypercarnivores based on dentition and *C. falconeri* has also been hypothesized to be a
146 hypercarnivore similar to modern gray wolves (Palmqvist et al. 1999). *Canis chihliensis* shares
147 some similarities with *Sinicuon dubius* (Tong et al. 2012). Furthermore, *C. chihliensis* is among
148 the largest *Canis* species of Eurasia in the early Pleistocene.
149
150 **Dental Fracture and Inflammations as Related to Bone-crushing and Hypercarnivory**. The
151 left dentary (IVPP V17755.11) and right dentary (IVPP V17755.12) belong to the same

152   individual. The left dentary (Fig. 1.A1-4) has c, p1-3 and m2-3 intact, while the crown of p4 and
153   trigonid of m1 and mesial root of m1 are fractured and lost, apparently due to injuries suffered
154   during life. Both root fragments of p4 are retained. On m1 only the talonid is preserved. Note on
155   Fig 1.A1 that the alveolar bone in the region of the missing mesial root of m1 shows no residual
156   socket, which indicates antemortem bone remodeling. This is consistent with the radiographic
157   evidence of periapical bone resorption associated with the apices of the retained roots of p4 and
158   the distal root of m1 (described below). There is also partial loss of the enamel on c and m1 and
159   fracturing of the crowns of p2, p3, and root of m1. The pulp cavities of p4 and m1 are exposed.
160   The dentin of all teeth is stained brown. All remaining cusps are moderately worn.
161   There are multiple fractures of the buccal and lingual cortical surfaces of the mandible
162   primarily in the regions of p2-p3, m1-m2, and the posterior surface of the mandibular ramus
163   including the condylar process. All fractures appear to be postmortem as suggested by the
164   absence of any repair.
165   There is loss of the cortical bone on the alveolar ridge in the regions of p3, p4, and m1. This
166   was most likely caused by periodontitis in vivo although there may have also been some
167   postmortem fracturing of the alveolar bone around m1.
168   The right dentary (Fig. 1.B1-4) preserves i2-3, c, p1-4, and m1-2 in situ; the crown of m3 is
169   missing, but one root tip remains deep in the alveolus. The crown of m1 is brownish due to loss
170   of most of the enamel cap, and with the pulp cavity exposed; m2 was broken during excavation;
171   and other teeth are moderately worn. There are multiple fractures of the buccal and lingual
172   cortical bone, predominantly in the regions of p1 and m2, that are postmortem defects.
173   The right dentary also suffered serious injury. The bone surrounding the m1 root is
174   perforate on the buccal cortex (purple arrow on Fig. 1.B4) by an apparent fistula and there is
175   extensive loss of alveolar bone over the buccal aspect of the mesial root of m1 (red arrow on Fig.
176   1.B4). The buccal cortical surface is porous adjacent to p4 and m1 (white arrows on Fig. 1.B2).
177   This is most likely the result of increased number and size of vascular canals associated with
178   inflammation in this region.
179
180   **Radiographic Observation.** The radiographic images of the right and left hemi-mandibles
181   reveal periapical bone loss (rarefying osteitis) (blue arrows on Figs. 1.A4 and 1.B4) associated
182   with exposed pulp cavities, a periodontal pocket between the right p4 and m1 (red arrow on Fig.
183   1.B4), and an apparent fistula from the periodontal pocket to the surface (purple arrows on Figs.
184   1.B2 and 1.B4).
185
186   **Interpretation and Implications for Dental Injury.** IVPP V17755 suffered from repeated
187   dental injuries in similar locations on both left and right sides. Although both lever models and *in*
188   *vivo* experimentation (Ellis et al. 2008) show that biting forces are greatest on the posterior-most
189   molars, patterns of tooth wear suggest that the lower p4-m1 are used more frequently than more
190   posterior molars (Tseng & Wang 2010; Wang et al. 2008; Werdelin 1989), although in the case
191   of the most hypercarnivorous canid, *Lycaon*, bone consumption may be at a more posterior

192   location (Van Valkenburgh 1996). Dental modifications for bone consumption in fossil
193   borophagine canids are most apparent in the p4-m1 region, indicating that this was the location
194   of most bone-cracking behavior (Wang et al. 1999). We interpret the loss of the left p4-m1 in
195   IVPP V17755 as owing to bone-cracking—the p4 and m1 are the largest lower cheek teeth in
196   *Canis* and their loss must have been inflicted by a strong biting force. Preservation of the roots of
197   both the p4 and the m1 trigonid (Fig. 1.A4) suggests tooth fracture from a strong bite and/or
198   encountering hard objects. The alveolar bone in the region of the missing m1 mesial root
199   eventually healed, but the periapical infections associated with both retained root fragments of p4
200   and the distal root of m1 still show active lesions.
201   The need for bone-crushing in IVPP V17755 would have continued during and after the
202   healing of the wounds on the left side. Accordingly, the right p4-m1 suffered excessive wear,
203   likely to compensate for the loss of the same function on the left side. Again, we infer that the
204   heavy wear is due to chewing on bones. The wear on the crown of m1 led to exposure of the pulp
205   chamber through two pulp horns in the mesial cusp and directly to the periapical lesions
206   (abscess) (blue arrows in Figs. 1.A4 and 1.B4). This lesion grew sufficiently that it created a
207   fistula to the buccal surface of the dentary to allow drainage of pus. It is also likely that excessive
208   use on the right side led to bone splinters (shards, fragments) being imbedded into the gum tissue
209   between p4 and m1, causing a periodontal pocket.
210   The above scenario suggests prolonged and possibly repeated injuries and infections, first to
211   the left p4-m1 (possibly broken in a single bite), and then to the right jaw perhaps after the left
212   side had partially healed. Such a scenario is consistent with a hypercarnivorous dentition in *C.*
213   *chihliensis* frequently used for bone consumption, as also seen in late Pleistocene European *Cuon*
214   (Iurino & Sardella 2014). Bone-crushing behavior in canids has been linked to collaborative
215   hunting and competitive consumption of carcasses within the same family group of predators
216   (Wang et al. 2008; Wang et al. 2018). Such a behavior is especially prevalent among large,
217   hypercarnivorous canids, and Van Valkenburgh et al. (2019) recently linked high tooth fractures
218   in extant gray wolves to limited prey availability.
219
220   **Comparison to Rancho La Brea *Canis dirus*.** In Pit 61/67 alone, 35 dentaries of adult age (14
221   left, 21 right)—out of 64 pathological adult dentaries (25 left, 39 right; 55%) and 617 dentaries
222   total (both pathological and non-pathological; 5.7%)—exhibit dental injuries similar to those in
223   the Nihewan *C. chihliensis* dentaries examined in this current study (Fig. S3). Across Rancho La
224   Brea deposits, abscesses and alveolar resorption likely due to infection were preserved in 43%
225   (Pit 16) to 77% (Pit 3) of pathological dentaries (Fig. 2.A). Most of the remaining pathological
226   dentaries also preserved dental anomalies, predominantly supernumerary teeth (particularly in
227   the first and second premolars) or a missing lower first premolar (p1) and/or third molar (m3).
228   Because both the p1 and m3 (Balisi et al. 2018; Buchalczyk et al. 1981; Wang 1994) vary in their
229   presence among canids, we excluded anomalies in these teeth from our comparison with
230   Nihewan *C. chihliensis*. Across 200 *C. dirus* jaws (both left and right) bearing abscesses and
231   alveolar infections, the lower first molar or carnassial showed the highest frequency of injury (87

232   total specimens with m1-associated injuries), likely inflicted by bone-crushing during the
233   consumption of prey, followed by the second premolar (79 total specimens with p2-associated
234   injuries), likely the result of biting and killing while chasing prey or in fighting with conspecifics
235   or competitors of other species (Fig. 2.B). The fourth premolar was the third most frequently
236   injured tooth (57 specimens); often, it was injured in conjunction with the lower first molar (34
237   specimens), as in the case of *C. chihliensis*. As *C. dirus* is a predator widely recognized to have
238   had a forceful bite capable of processing bone (Anyonge & Baker 2006; Brannick et al. 2015;
239   Van Valkenburgh & Hertel 1993), the high frequency of injury in its p4-m1 complex—similar to
240   that found in the specimens of *C. chihliensis* examined here—supports the inference that *C.*
241   *chihliensis* also processed bone using p4 and m1.
242
243   **Tibia Fracture**. A normal left tibia (IVPP V18139.21) and pathologic right tibia (IVPP
244   V18139.20) of *Canis* are present in the collection from Shanshenmiaozui (SSMZ). The
245   pathologic tibia has healed fractures at the lower one-third of the shaft. Compared with the
246   normal tibia on the left side (Fig. 3), the pathologic tibia is stouter; it is much broader distally,
247   especially at the fracture site, and is shorter, the maximum length for the normal tibia being
248   181.6 mm, in contrast to the pathologic one at 166.5 mm (Table 1). In addition, the nutrient
249   foramen is much more enlarged in the pathologic tibia. The partially healed bone has a rough and
250   porous surface (callus).
251   The porous bone surface indicates that the periosteal vessels also took part in the repair of
252   the fracture, which penetrated into the hard callus. Because the woven/primary bone is not
253   replaced with secondary lamellar bone, this individual did not survive to the stage of lamellar
254   bone formation, i.e. the fracture healing stage 6 by Edge-Hughes & Nicholson (2007).
255
256   **Foreshortening of tibia.** The pathologic tibia has fused overlapping components with
257   remodeling starting 4 cm from the proximal surface and extending throughout the length.
258   Accentuation (irregularities) of the enthesial region at the lateral margin of the tibial plateau
259   suggests increased stress at the proximal tibial-fibular joint. The tibia widens abnormally starting
260   6 cm distal to proximal surface, with concurrent alteration of surface color and texture,
261   continuing on to the fused distal component of the tibial fracture, where surface filigree reaction
262   (characteristic of infection) is more prominent. There are increased vascular markings at the
263   junction of proximal and middle third (related to current length) of the tibia. A shallow groove
264   identifies the original demarcation of the fracture components now fused. The fibula was also
265   fractured, and residual components are noted at the distal 6 cm. A linear defect is noted at the
266   mid-portion of the tibia, slightly medial to the sagittal line. It appears to be perforated in a
267   manner more suggestive of vasculature than of draining sinuses. It may be the residua of the
268   fracture. If so, it would mean that the injury not only caused fracture, separation and overlap of
269   components, but also caused a "splintering" or at least slight separation of the distal portion of
270   the proximal component. Increased vascularity is noted 2 cm from the distal end of the tibia.
271

272   **X-ray Examination.** Increased density of the medial tibial plateau is noted. If not related to an
273   artifact (e.g., glued component), this is suggestive of a healed, minimally displaced fracture.
274   There clearly is a displaced distal fracture, fused incompletely with overlap. The curvature of the
275   distal portion of the proximal component suggests torsion of the components related to each
276   other. Several layers of periosteal reaction are noted, with partial disruption of subjacent cortex.
277   The distal fibula is fused to the tibia, with focal loss of margin definition. Irregular cavities are
278   noted in the distal portion of the proximal component of the fracture and adjacent to the distal
279   junction of the tibia and fibula. Both contain radio-dense material. This suggests that this was a
280   compound fracture, with skin breach and exposure to environmental contamination. The fracture
281   was incompletely stabilized during the healing process, with continued movement of the
282   components.

283

284   **CT Scan.** The CT images show clearly that it was a comminuted fracture, and all three pieces of
285   the fractures are displaced, which resulted in the division of the medullary cavity into three
286   chambers whose broken ends were enclosed by callus or woven bones (Fig. 4.B1-2, C1-2).
287   CT longitudinal sections slice 1 (Fig. 4.B1-2) – There is a focal area of trabecular loss just
288   distal to the proximal epiphyseal plate. It is irregularly ellipsoid in shape and contains slightly
289   thickened bone "fragments" of apparently increased density. Increased density is noted in the
290   subsequent proximal fracture component. Periosteal reaction is noted with multiple focal areas of
291   trabecular loss, bounded by sclerotic margins, characteristic of abscesses. There is massive loss
292   of cortical bone in the region of fragment fusion. Fibular fusion with a distal radio-dense
293   inclusion is noted. Presence of foreign bodies is consistent with the diagnosis of a compound
294   fracture.
295   CT longitudinal sections slice 2 (Fig. 4.C1-2) – There is an area of increased density at the
296   median tibial plateau noted on the x-ray. The CT shows this area to be separated by a fracture
297   line from subjacent bone. The trabecular pattern is denser. The lateral portion of the proximal
298   epiphyseal plate is partially preserved, in contrast to the medial portion, which cannot be
299   distinguished from the epiphysis. This appears to be a non-displaced fracture through the
300   epiphyseal plate, only affecting a portion of that plate.
301   There is a linear focal disruption (partially occluded at the surface) of the medial aspect at
302   the midpoint of the current length and a U-shaped defect (also seen in CT slice 1) with thickened
303   margins at the distal fifth. The latter could represent a draining abscess, although the former
304   suggests the possibility of a penetrating injury. Radio-dense inclusions are noted, perhaps
305   representing environmental exposure at time of injury. The surface imperfection seen on the
306   reconstructed tibial image (Fig. 4.A) may be a CT averaging artifact. A series of 8 cross sections
307   (Figs. 4D.1-8) allows comparisons of healthy cancellous (D1), healthy cortical (D2-3), and
308   injured and healed bones (D4-8).

309

310   **Interpretation, Comparison, and Implications for Limb Injury.** That the injury, plus the
311   subsequent infections, suffered by IVPP V18139 must have been devastating seems not in doubt.

312   The displacement of the right hindlimb and the pain associated with a compound fracture with
313   skin breach and exposure to environmental contamination all but rule out hunting activities. For
314   modern domestic dogs of more than 1 year of age, fracture healing can take 7 weeks to 1 year
315   (Edge-Hughes & Nicholson 2007). It is safe to assume that healing of the open fractures in IVPP
316   V18139 without medical intervention (broken bones not re-aligned nor cast to immobilize
317   wounds) would take a considerable amount of time, much longer than its metabolic reserve can
318   sustain. Such a long-term survival by an injured wolf requiring a high degree of meat
319   consumption thus suggests family care and collaborative hunting.
320   In addition to abnormalities in the jaws and dentition, the Rancho La Brea dire wolf
321   collection has numerous healed fractures in the limb bones (Moodie 1918; Shaw & Howard
322   2015; Stock 1930; Ware 2005). Again focusing on Pit 61/67, which has a minimum number of
323   371 dire wolf individuals, Brown et al. (2017) showed that frequencies of traumatic injury—
324   including healed fractures—were higher than expected for most limb bones, especially the tibia.
325   Surveying dire wolf tibiae across all Rancho La Brea deposits, we found 11 specimens (5 left, 6
326   right) of 251 total pathologic tibiae (4.38%) to have suffered an oblique fracture with
327   foreshortening similar to that in IVPP V18139 (Fig. S4). In studies of modern Saskatchewan
328   gray wolves and sympatric coyotes, such bone fractures—which likely resulted from conflicts
329   with large prey—were found to be more common in wolves than in coyotes, a difference thought
330   to result from wolves' tendency to prey on larger animals like moose (Wobeser 1992). Similarly,
331   Rancho La Brea preserves no fractured and healed tibiae belonging to the coyote—which is also
332   found abundantly in the Pleistocene to Holocene-age asphalt seeps—though this lack may be
333   confounded by a coyote sample size an order of magnitude smaller than that of the dire wolf.

Discussion

335   Life is not easy for large predators. In modern canids, hypercarnivory is almost always
336   associated with social hunting, such as in the gray wolves (*Canis lupus*), African hunting dogs
337   (*Lycaon pictus*), and Asiatic dholes (*Cuon alpinus*). Of these, the latter two most
338   hypercarnivorous species almost invariably hunt cooperatively, whereas gray wolves regularly,
339   but not exclusively, hunt together for large prey (Macdonald 1983). Group hunting by these
340   highly social canids offers apparent advantages that are otherwise unavailable to individual
341   hunters, such as the ability to bring down prey much larger than the predators themselves, plus
342   coordinated attacks that seal off escape routes as well as relaying strategies that lessen the burden
343   of individual hunters. These strategies are especially critical to canids because, unlike felids,
344   canids never evolved fully retractile claws that are effective weapons for grappling and subduing
345   prey (Wang 1993). Therefore, for canids, group hunting is not optional, as it is for large cats
346   (only the lions are social hunters), once canids have crossed the critical body mass threshold of
347   about 21 kg above which energetic costs necessitate feeding on large prey (Carbone et al. 1999).
348   For canids, it is possible that this body size threshold may even be substantially lowered as in the
349   case of the Asiatic dholes (10-13 kg) that have the most extremely hypercarnivorous dentitions

350   among living canids (Cohen 1978). The Nihewan *Canis chihliensis* is larger than the dholes
351   (13.7–16.8 kg based on femur shaft diameter; ~21.2 kg based on the mean of m1 length).
352   Social hunting is characteristic of large canids, hyaenids, and some felids. Such behavior
353   has important implications not only in the social organizations of large carnivorans but also in
354   their trophic relationships and diet. Among large, hypercarnivorous living canids, the gray wolf
355   (*Canis lupus*) is the best studied in its pack hunting behavior. The basic social unit is the mated
356   pair; prey size is a factor in pack sizes, which range from a few up to 20 individuals, with the
357   largest packs preying on bison and moose and smaller packs preying on deer (Mech & Boitani
358   2003). Social hunting, however, may not always be the most efficient in terms of food intake per
359   wolf because the packs must share their proceeds (Thurber & Peterson 1993). The formation of
360   packs, therefore, offers the opportunity to kill prey too large to tackle by one individual alone, as
361   well as the opportunity both to better defend kills against carcass theft and to steal carcasses from
362   larger predators (Carbone et al. 1997; Eaton 1979; Van Valkenburgh 2001).
363   It has been long known that large *Canis* from the Nihewan Basin includes individuals with
364   highly trenchant lower molars (Teilhard de Chardin & Piveteau 1930). Hypercarnivorous
365   characteristics (dominance of cutting edge of m1 trigonid and enlargement of hypoconid at the
366   expense of entoconid, along with reductions of posterior molars) in *C. chihliensis* are variable
367   (Tong et al. 2012) but strongly converge on the morphology of living African hunting dogs and
368   Asiatic dholes (Fig. 5). Such a dental morphology is commonly associated with emphasis in
369   slicing meat using the sharp carnassial blades. Trenchant molars thus correlate well with
370   hypercarnivory (Crusafont-Pairó & Truyols-Santonja 1956), i.e., tendency to consume meat
371   exclusively, which also drives the evolution of larger body size as a macroevolutionary ratchet
372   (Van Valkenburgh et al. 2004).
373   Wolves have a dangerous life as long-distance pursuit predators. The traumas and infections
374   inflicted on *Canis chihliensis* likely are related to hunting behavior, feeding strategies, and
375   predator-prey interactions, as has also been suggested for other extinct carnivores (Shaw & Ware
376   2018). Healing of such devastating injuries is also a testimony to its survival for long periods of
377   time during which the ability to hunt must have been seriously limited or nonexistent, suggesting
378   that some kind of assisted living was necessary. Debilitating bone diseases in the Pleistocene
379   apex predator *Smilodon*, which is even more hypercarnivorous than canids, have also been used
380   to argue for social or gregarious behaviors (Akersten 1985; Heald 1989; Shaw 1992a; Shaw
381   1992b; Van Valkenburgh 2009; Van Valkenburgh & Sacco 2002) although the pathology-
382   sociality link has been challenged (McCall et al. 2003). Schleidt & Shalter (2004) also noted that
383   social predators should have more healed injuries than solitary predators. Often infirm animals
384   are allowed to feed on group kills, as observed in spotted hyaenas and African wild dogs.
385   Whereas sociality in sabertooth cats has been questioned given its rarity among extant large
386   felids, all of which are capable of killing on their own, pack hunting in dog-like carnivorans
387   (wolves, hunting dogs, dholes, hyenas) is the dominant mode of predation and is primarily driven
388   by the necessity of overcoming larger prey. Dental morphology and pathology in our Nihewan
389   *Canis chihliensis* strongly suggest processing of hard food (bone cracking), which is commonly

390 associated with hypercarnivory and pack hunting in large canids. Although the massive, healed
391 tibial fracture may not be a definitive indication of social care, such a devastating injury is highly
392 suggestive of the necessity of food provisioning that only social groups can offer, as has been
393 similarly proposed from an early Pleistocene Spanish record of *C. falconeri* (Palmqvist et al.
394 1999). With this new record from Nihewan, we extend the history of *Canis* sociality to the early
395 Pleistocene, and—by phylogenetic extension, given the probable divergence date between the
396 lineages leading to *Canis chihliensis* and the social dire wolf *Canis dirus*—likely to the Pliocene
397 as well.
398   Arguably the most definitive (though still correlative) pathological evidence to support
399 sociality in *Canis chihliensis* would be a significant prevalence of similar injuries not only in the
400 extinct *Canis dirus* but in the three extant hypercarnivorous canines whose pack-hunting
401 behavior can be observed directly, in contrast to a low prevalence of similar injuries in non-pack-
402 hunting carnivoran species. However, one common challenge in predator paleopathology is the
403 lack of sufficient samples of large-predator post-crania relative to crania in museum collections
404 of living mammals. This limitation—and the corresponding lack of published systematic
405 pathological surveys across large sample sizes within and among extant species—prevents
406 statistically robust inferences of injury prevalence in extant wild animals. When isolated cases
407 are available, lack of field documentation on behaviors related to pathological specimens also
408 hampers interpretations. Such deficiencies make it difficult to ground-truth inferences of extinct
409 behaviors based on extant relatives, even where large samples of extinct predators are available
410 (Brown et al. 2017). While such a systematic comparative survey exceeds the scope of the
411 current paper, future studies that calculate injury prevalence across large museum and zoo
412 collections of extant species of known behavior (e.g., Rothschild et al. 1998) would bolster
413 inferences of extinct behavior based on skeletal injuries.
414   As knowledge of the fossil history of hypercarnivorous canids in the Plio-Pleistocene of
415 Eurasia increases, more complexity than has been previously assumed is now emerging, both in
416 its chronology and its morphologic diversity. Recent molecular studies placed *Cuon* and *Lycaon*,
417 two of the most hypercarnivorous living canids, near the base of the *Canis* clade (Lindblad-Toh
418 et al. 2005), in contrast to morphological analysis suggesting that hypercarnivorous forms are at
419 the terminal end of the canine phylogeny (Tedford et al. 1995; Tedford et al. 2009). If the
420 molecular relationship is correct, then records of *Cuon* and *Lycaon* are expected to be at least as
421 old, if not older, than that of many species of *Canis*. This new record pushes back the first
422 occurrence of social care, and pack hunting by extension, by about 1.7 million years to when
423 early *Homo erectus* was first recorded in Asia (Ao et al. 2013; Zhu et al. 2004). This record is
424 important because it coincides with the initial diversification of the large canids (such as *Canis*
425 and *Lycaon*), also known as the Wolf Event (Azzaroli 1983; Sardella & Palombo 2007), and is
426 associated with pack hunting behavior by large carnivorans in increasingly open habitats.
427   Although records of early wolves have been pushed back slightly (Martínez-Navarro et al.
428 2009; Rook & Martínez-Navarro 2010; Sardella & Palombo 2007), the wolf event is essentially
429 confined to the Early Pleistocene, i.e., Late Pliocene before recent redefinition (Gibbard et al.

430   2010). A recent new Tibetan record in the Middle Pliocene, *Sinicuon* cf. *S. dubius*, seems to
431   suggest that hypercarnivorous canines may have predated the genus *Canis* (Wang et al. 2014).
432   Whatever the detailed relationships of these records, it seems clear that hyper-predators, such as
433   large wolves and hunting dogs, were associated with the increasingly open habitats in Eurasia
434   during the onset of the Pleistocene. In this background of large-canine radiation at the beginning
435   of the Ice Age, our new record of a pathological wolf from the Early Pleistocene of Nihewan
436   hints at pack hunting as a major step toward social collaboration while procuring food and, as
437   such, signals a major step in the evolution of large canids.
438

Acknowledgments

440   The authors wish to express their thanks to the following people and organizations for their help:
441   Han F., Sun B. Y., Lü D., Sun J. J., Xu Z. J., Qiu Z. W., Wang Q. Y., Sun B. H., Hu N., Liu X.
442   T. & Yin C. for participating the fieldwork; Xie F. of HPICR, Zhao W. J. of NNNRM and Hou
443   W. Y. of NM for help during excavations; Qiu Z. X., Wei Q. for sharing bibliographies and/or
444   for fruitful discussions; Hou Y. M. for CT scanning; F. Heald and C. Shaw for initial diagnosis
445   and assembly of the Rancho La Brea pathology collection; A. Farrell and G. Takeuchi for
446   Rancho La Brea collections access; B. Van Valkenburgh for thoughtful critique.
447

References

449   Akersten WA. 1985. Canine function in *Smilodon* (Mammalia: Felidae: Machairodontinae).
450   *Natural History Museum of Los Angeles County Contributions in Science* 356:1-22.
451   Anyonge W, and Baker A. 2006. Craniofacial morphology and feeding behavior in *Canis dirus*,
452   the extinct Pleistocene dire wolf. *Journal of Zoology* 269:309-316.
453   Anyonge W, and Roman C. 2006. New body mass estimates for *Canis dirus*, the extinct
454   Pleistocene dire wolf. *Journal of Vertebrate Paleontology* 26:209-212.
455   Ao H, An Z, Dekkers MJ, Li Y, Xiao G, Zhao H, and Qiang X. 2013. Pleistocene
456   magnetochronology of the fauna and Paleolithic sites in the Nihewan Basin: Significance
457   for environmental and hominin evolution in North China. *Quaternary Geochronology*
458   18:78-92. http://dx.doi.org/10.1016/j.quageo.2013.06.004
459   Azzaroli A. 1983. Quaternary mammals and the "end-Villafranchian" dispersal event — A
460   turning point in the history of Eurasia. *Palaeogeography, Palaeoclimatology,*
461   *Palaeoecology* 44:117-139. http://dx.doi.org/10.1016/0031-0182(83)90008-1
462   Balisi M, Wang X, Sankey J, Biewer J, and Garber D. 2018. Fossil canids from the Mehrten
463   Formation, Late Cenozoic of Northern California. *Journal of Vertebrate Paleontology*
464   36:e1405009. 10.1080/02724634.2017.1405009
465   Brannick AL, Meachen JA, and O'Keefe FR. 2015. Microevolution of jaw shape in the dire wolf,
466   *Canis dirus*, at Rancho La Brea. *Natural History Museum of Los Angeles County Science*
467   *Series* 42:23-32.

468 Brown C, Balisi M, Shaw CA, and Van Valkenburgh B. 2017. Skeletal trauma reflects hunting
469   behaviour in extinct sabre-tooth cats and dire wolves. *Nature Ecology & Evolution*
470   1:0131. 10.1038/s41559-017-0131
471 Buchalczyk T, Dynowski J, and Szteyn S. 1981. Variations in number of teeth and asymmetry of
472   the skull in the wolf. *Acta Theriologica* 26:23-30.
473 Carbone C, Du Toit JT, and Gordon IJ. 1997. Feeding success in African Wild Dogs: Does
474   kleptoparasitism by spotted hyenas influence hunting group size? *Journal of Animal*
475   *Ecology* 66:318-326. 10.2307/5978
476 Carbone C, Mace GM, Roberts SC, and Macdonald DW. 1999. Energetic constraints on the diet
477   of terrestrial carnivores. *Nature* 402:286-288.
478 Carbone C, Maddox T, Funston PJ, Mills MGL, Grether GF, and Valkenburgh BV. 2009.
479   Parallels between playbacks and Pleistocene tar seeps suggest sociality in an extinct
480   sabretooth cat, *Smilodon. Biology Letters* 5:81-85. doi:10.1098/rsbl.2008.0526
481 Chen X. 2018. Taphonomic study of Early Pleistocene Shanshenmiaozui fossil site in Nihewan
482   Basin, North China Ph.D. University of Chinese Academy of Sciences.
483 Chen X, and Tong H-w. 2015. Taphonomy of the *Canis chihliensis* fossil assemblage from the
484   Shanshenmiaozui Site, Nihewan Basin. *Acta Anthropologica Sinica* 34:553-564.
485 Cohen JA. 1978. *Cuon alpinus. Mammalian Species* 100:1-3.
486 Crusafont-Pairó M, and Truyols-Santonja J. 1956. A biometric study of the evolution of fissiped
487   carnivores. *Evolution* 10:314-332.
488 Eaton RL. 1979. Interference competition among carnivores: A model for the evolution of social
489   behavior. *Carnivore* 2:9-16.
490 Edge-Hughes L, and Nicholson H. 2007. 13, Canine treatment and rehabilitation. In: McGowan
491   CM, Goff L, and Stubbs N, eds. *Animal Physiotherapy: Assessment, Treatment and*
492   *Rehabilitation of Animals*. Oxford: Blackwell Publishing, 207-234.
493 Ellis JL, Thomason JJ, Kebreab E, and France J. 2008. Calibration of estimated biting forces in
494   domestic canids: comparison of post-mortem and in vivo measurements. *Journal of*
495   *Anatomy* 212:769-780. 10.1111/j.1469-7580.2008.00911.x
496 Gibbard PL, Head MJ, Walker MJC, Alloway B, Beu AG, Coltorti M, Hall VM, Liu J-q,
497   Knudsen KL, Van Kolfschoten T, Litt T, Marks L, McManus J, Partridge TC, Piotrowski
498   JA, Pillans B, Rousseau D-D, Suc JP, Tesakov AS, Turner C, and Zazo C. 2010. Formal
499   ratification of the Quaternary System/Period and the Pleistocene Series/Epoch with a
500   base at 2.58 Ma. *Journal of Quaternary Science* 25:96-102. 10.1002/jqs.1338
501 Gipson PS, Ballard WB, and Mech RMND. 2000. Accuracy and precision of estimating age of
502   gray wolves by tooth wear. *Journal of Wildlife Management* 64:752-758.
503 Hartstone-Rose A, Dundas RG, Boyde B, Long RC, Farrell AB, and Shaw CA. 2015. The bacula
504   of Rancho La Brea. *Natural History Museum of Los Angeles County Science Series*
505   42:53-63.
506 Heald FP. 1989. Injuries and diseases in *Smilodon californicus* Bovard, 1904 (Mammalia
507   Felidae) from Rancho la Brea, California. *Journal of Vertebrate Paleontology* 9:24A.
508 Hemmer H. 1978. Considerations on sociality in fossil carnivores. *Carnivore* 1:105-107.
509 Iurino DA, and Sardella R. 2014. Medical CT scanning and the study of hidden oral pathologies
510   in fossil carnivores. *Paläontologische Zeitschrift* 89:251-259.
511 Lawler DF, Widga C, and Smith GK. 2017. Observations of the acetabulum and proximal femur
512   of the dire wolf (*Canis dirus*, Leidy 1854). *Journal of Veterinary Anatomy* 10:73-83.

513 Lindblad-Toh K, Wade CM, Mikkelsen TS, Karlsson EK, Jaffe DB, Kamal M, Clamp M, Chang
514   JL, Kulbokas EJ, Zody MC, Mauceli E, Xie X, Breen M, Wayne RK, Ostrander EA,
515   Ponting CP, Galibert F, Smith DR, deJong PJ, Kirkness E, Alvarez P, Biagi T, Brockman
516   W, Butler J, Chin C-W, Cook A, Cuff J, Daly MJ, DeCaprio D, Gnerre S, Grabherr M,
517   Kellis M, Kleber M, Bardeleben C, Goodstadt L, Heger A, Hitte C, Kim L, Koepfli K-P,
518   Parker HG, Pollinger JP, Searle SMJ, Sutter NB, Thomas R, Webber C, and Lander ES.
519   2005. Genome sequence, comparative analysis and haplotype structure of the domestic
520   dog. *Nature* 438:803-819.
521 Liu P, Wu Z, Deng C, Tong H, Qin H, Li S, Yuan B, and Zhu R. 2016. Magnetostratigraphic
522   dating of the Shanshenmiaozui mammalian fauna in the Nihewan Basin, North China.
523   *Quaternary International* 400:202-211. https://doi.org/10.1016/j.quaint.2014.09.024
524 Macdonald DW. 1983. The ecology of carnivore social behaviour. *Nature* 301:379-384.
525   10.1038/301379a0
526 Martínez-Navarro B, Belmaker M, and Bar-Yosef O. 2009. The large carnivores from 'Ubeidiya
527   (early Pleistocene, Israel): biochronological and biogeographical implications. *Journal of
528   Human Evolution* 56:514-524. http://dx.doi.org/10.1016/j.jhevol.2009.02.004
529 McCall S, Naples V, and Martin L. 2003. Assessing behavior in extinct animals: Was *Smilodon*
530   social? *Brain, Behavior and Evolution* 61:159-164. 10.1159/000069752
531 Mech LD, and Boitani L. 2003. Wolf social ecology. In: Mech LD, and Boitani L, eds. *Wolves,*
532   *Behavior, Ecology, and Conservation*. Chicago: University of Chicago Press, 1-34.
533 Merriam JC. 1912. The fauna of Rancho la Brea, Part II. Canidae. *Memoirs of the University of*
534   *California* 1:218-262.
535 Mescher AL. 2018. *Junqueira's Basic Histology: Text and Atlas, 15th Edition*. New York:
536   McGraw-Hill Education.
537 Moodie RL. 1918. Paleontological evidences of the antiquity of disease. *The Scientific Monthly*
538   7:265-281.
539 Palmqvist P, Arribas A, and Martínez-Navarro B. 1999. Ecomorphological study of large canids
540   from the lower Pleistocene of southeastern Spain. *Lethaia* 32:75-88.
541 Qiu Z-x. 2000. Nihewan fauna and Q/N boundary in China. *Quaternary Sciences* 20:154-163.
542 Rook L. 1994. The Plio-Pleistocene Old World *Canis* (*Xenocyon*) ex gr. *falconeri*. *Bollettino*
543   *della Società Paleontologica Italiana* 33:71-82.
544 Rook L, and Martínez-Navarro B. 2010. Villafranchian: The long story of a Plio-Pleistocene
545   European large mammal biochronologic unit. *Quaternary International* 219:134-144.
546   http://dx.doi.org/10.1016/j.quaint.2010.01.007
547 Rothschild BM, Rothschild C, and Woods RJ. 1998. Inflammatory arthritis in large cats: An
548   expanded spectrum of spondyloarthropathy. *Journal of Zoo and Wildlife Medicine*
549   29:279-284.
550 Rothschild BM, Wang X, and Shoshani J. 1994. Spondyloarthropathy in proboscideans. *Journal*
551   *of Zoo and Wildlife Medicine* 25:360-366.
552 Sardella R, and Palombo MR. 2007. The Pliocene-Pleistocene boundary: which significance for
553   the so called "Wolf Event"? Evidences from Western Europe. *Quaternaire* 18:65-71.
554 Schleidt WM, and Shalter MD. 2004. Co-evolution of humans and canids, An alternative view of
555   dog domestication: Homo Homini Lupus? *Evolution and Cognition* 9:57-72.
556 Shaw CA. 1992a. Old wounds: the paleopathology of Rancho la Brea. *Terra* 31:17.
557 Shaw CA. 1992b. The sabertoothed cat. *Terra* 31:26.

558 Shaw CA, and Howard C. 2015. Facial asymmetry in the sabercat (*Smilodon fatalis*) and wolf
559   (*Canis dirus*) from Rancho la Brea, Los Angeles, California. *PaleoBios* 32:15.
560 Shaw CA, and Ware CS. 2018. Chapter 11, *Smilodon* paleopathology: A summary of research at
561   Rancho La Brea. In: Werdelin L, McDonald HG, and Shaw CA, eds. *Smilodon, the*
562   *Iconic Sabertooth*. Baltimore: Johns Hopkins University Press, 196-206.
563 Sotnikova MV. 2001. Remains of Canidae from the lower Pleistocene site of Untermassfeld. In:
564   Kahlke R-D, ed. *Das Pleistozäne von Untermassfeld bei Meiningen (Thüringgen) Teil 2*.
565   Mainz: Römisch-Germanischen Zentralmuseums, 607-632.
566 Stock C. 1930. Rancho la Brea: a record of Pleistocene life in California. *Los Angeles County*
567   *Museum of Natural History Science Series* 20:1-81.
568 Summer-Smith G. 1966. Observations on epiphyseal fusion of the canine appendicular skeleton.
569   *Journal of Small Animal Practice* 7:303-311.
570 Tedford RH, Taylor BE, and Wang X. 1995. Phylogeny of the Caninae (Carnivora: Canidae): the
571   living taxa. *American Museum Novitates* 3146:1-37.
572 Tedford RH, Wang X, and Taylor BE. 2009. Phylogenetic systematics of the North American
573   fossil Caninae (Carnivora: Canidae). *Bulletin of the American Museum of Natural History*
574   325:1-218.
575 Teilhard de Chardin P, and Piveteau J. 1930. Les mammifères fossiles de Nihowan (Chine).
576   *Annales de Paléontologie* 19:1-134.
577 Thurber JM, and Peterson RO. 1993. Effects of population density and pack size on the foraging
578   ecology of gray wolves. *Journal of Mammalogy* 74:879-889. 10.2307/1382426
579 Tong H-w, and Chen X. 2015. On newborn calf skulls of Early Pleistocene *Mammuthus*
580   *trogontherii* from Shanshenmiaozui in Nihewan Basin, China. *Quaternary International*
581   406, Part B:57-69. http://dx.doi.org/10.1016/j.quaint.2015.02.026
582 Tong H-w, Chen X, and Zhang B. 2017. New fossils of *Bison palaeosinensis* (Artiodactyla,
583   Mammalia) from the steppe mammoth site of Early Pleistocene in Nihewan Basin, China.
584   *Quaternary International* 445:250-268. https://doi.org/10.1016/j.quaint.2016.07.033
585 Tong H-w, Chen X, and Zhang B. 2018. New postcranial bones of *Elasmotherium peii* from
586   Shanshenmiaozui in Nihewan Basin, Northern China. *Quaternaire* 29:195-204.
587 Tong H-w, Hu N, and Han F. 2011. A preliminary report on the excavation at the Early
588   Pleistocene fossil site of Shanshenmiaozui in Nihewan Basin, Hebei, China. *Quaternary*
589   *Sciences* 31:643-653.
590 Tong H-w, Hu N, and Wang X. 2012. New remains of *Canis chihliensis* (Mammalia, Carnivora)
591   from Shanshenmiaozui, a lower Pleistocene site in Yangyuan, Hebei. *Vertebrata*
592   *PalAsiatica* 50:335-360.
593 Tong H-w, and Wang X-m. 2014. Juvenile skulls and other postcranial bones of *Coelodonta*
594   *nihowanensis* from Shanshenmiaozui, Nihewan Basin, China. *Journal of Vertebrate*
595   *Paleontology* 34:710-724. 10.1080/02724634.2013.814661
596 Tong H-w, and Zhang B. 2019. New fossils of *Eucladoceros boulei* (Artiodactyla, Mammalia)
597   from Early Pleistocene Nihewan Beds, China. *Palaeoworld* 28:403-424.
598 Tseng ZJ, and Wang X. 2010. Cranial functional morphology of fossil dogs and adaptation for
599   durophagy in *Borophagus* and *Epicyon* (Carnivora, Mammalia). *Journal of Morphology*
600   271:1386–1398.
601 Van Valkenburgh B. 1990. Skeletal and dental predictors of body mass in carnivores. In:
602   Damuth J, and MacFadden BJ, eds. *Body Size in Mammalian Paleobiology: Estimation*
603   *and Biological Implications*. Cambridge: Cambridge University Press, 181-206.

604 Van Valkenburgh B. 1991. Iterative evolution of hypercarnivory in canids (Mammalia:
605   Carnivora): evolutionary interactions among sympatric predators. *Paleobiology* 17:340-
606   362.
607 Van Valkenburgh B. 1996. Feeding behavior in free-ranging, large African carnivores. *Journal*
608   *of Mammalogy* 77:240-254.
609 Van Valkenburgh B. 2001. The dog-eat-dog world of carnivores: a review of past and present
610   carnivore community dynamics. In: Stanford C, and Bunn HT, eds. *Meat-Eating and*
611   *Human Evolution*. Oxford: Oxford University Press, 101-121.
612 Van Valkenburgh B. 2009. Costs of carnivory: tooth fracture in Pleistocene and Recent
613   carnivorans. *Biological Journal of the Linnean Society* 96:68-81. 10.1111/j.1095-
614   8312.2008.01108.x
615 Van Valkenburgh B, and Hertel F. 1993. Tough times at La Brea: tooth breakage in large
616   carnivores of the late Pleistocene. *Science* 261:456-459.
617 Van Valkenburgh B, and Hertel F. 1998. The decline of North American predators during the
618   late Pleistocene. In: Saunders JJ, Styles BW, and Baryshnikov GF, eds. *Quaternary*
619   *Paleozoology in the Northern Hemisphere*. Springfield: Illinois State Museum, 357-374.
620 Van Valkenburgh B, Peterson RO, Smith DW, Stahler DR, and Vucetich JA. 2019. Tooth
621   fracture frequency in gray wolves reflects prey availability. *eLife* 8:e48628.
622   10.7554/eLife.48628
623 Van Valkenburgh B, and Sacco T. 2002. Sexual dimorphism, social behavior, and intrasexual
624   competition in large Pleistocene carnivorans. *Journal of Vertebrate Paleontology* 22:164-
625   169.
626 Van Valkenburgh B, Wang X, and Damuth J. 2004. Cope's rule, hypercarnivory, and extinction
627   in North American canids. *Science* 306:101-104.
628 Wang X. 1993. Transformation from plantigrady to digitigrady: functional morphology of
629   locomotion in *Hesperocyon* (Canidae: Carnivora). *American Museum Novitates* 3069:1-
630   23.
631 Wang X. 1994. Phylogenetic systematics of the Hesperocyoninae (Carnivora: Canidae). *Bulletin*
632   *of the American Museum of Natural History* 221:1-207.
633 Wang X, Li Q, and Xie G. 2014. Earliest record of *Sinicuon* in Zanda Basin, southern Tibet and
634   implications for hypercarnivores in cold environments. *Quaternary International* 355:3-
635   10. 10.1016/j.quaint.2014.03.028
636 Wang X, Tedford RH, and Antón M. 2008. *Dogs: Their Fossil Relatives & Evolutionary*
637   *History*. New York: Columbia University Press.
638 Wang X, Tedford RH, and Taylor BE. 1999. Phylogenetic systematics of the Borophaginae
639   (Carnivora: Canidae). *Bulletin of the American Museum of Natural History* 243:1-391.
640 Wang X, White SC, Balisi M, Biewer J, Sankey J, Garber D, and Tseng ZJ. 2018. First bone-
641   cracking dog coprolites provide new insight into bone consumption in *Borophagus* and
642   their unique ecological niche. *eLife* 7:e34773. 10.7554/eLife.34773
643 Ware CS. 2005. Disease, skeletal injury and trauma as possible behavior modifiers in the fossil
644   dire wolf *Canis dirus* (Canidae: Carnivora) from Rancho La Brea, California Ph.D.
645   Union Institute & University.
646 Werdelin L. 1989. Constraint and adaptation in the bone-cracking canid *Osteoborus* (Mammalia:
647   Canidae). *Paleobiology* 15:387-401.
648 Wobeser G. 1992. Traumatic, degenerative, and developmental lesions in wolves and coyotes
649   from Saskatchewan. *Journal of Wildlife Diseases* 28:268-275.

650   Zdansky O. 1924. Jungtertiäre carnivoren Chinas. *Palaeontologia Sinica Series C* 2:1-149.
651   Zhu R-x, Potts R, Xie F, Hoffman KA, Deng CL, Shi CD, Pan YX, Wang HQ, Shi RP, Wang
652   YC, Shi GH, and Wu NQ. 2004. New evidence on the earliest human presence at high
653   northern latitudes in northeast Asia. *Nature* 431:559-562.

654

Captions of Figures

656   **Figure 1 Two dentaries of the same individual of *Canis chihliensis*.** A, left dentary (IVPP
657   V17755.11); B, right dentary (IVPP V17755.12). A1, B1, occlusal views; A2, B2, buccal views;
658   A3, B3, lingual views; A4, B4, X-ray images. White arrows mark resorption of alveolar bone;
659   red arrows mark periodontal pocket, purple arrows indicate probable fistula from periodontal
660   pocket, blue arrows mark periapical infections associated with exposed pulp chambers, and white
661   arrows indicate porous cortical bone.

662   **Figure 2 Frequencies of dental injury in the mandible of Rancho La Brea dire wolves, *C.
663   dirus*.** A, numbers of specimens of adult age bearing injuries similar to those in *C. chihliensis*
664   (orange) compared with other dental injuries (gray). Most dental injuries in *C. dirus* involve
665   abscesses and alveolar resorption stemming from infection. B, categorization of dental injuries
666   by tooth position. The m1 shows the highest frequency of infection or injury, followed by p2 and
667   p4.

668   **Figure 3 Tibias of the same individual of *Canis chihliensis* from SSMZ, Nihewan.** A, normal
669   tibia of left side (IVPP V 18139.21); B, pathologic tibia of right side (IVPP V 18139.20); A1,
670   B1, anterior views; A2, B2, posterior views; A3, B3, medial views; A4, B4, lateral views. NF:
671   nutrient foramen.

672   **Figure 4 CT scan images of the pathologic right tibia of *Canis chihliensis* (V18139-20) from
673   SSMZ, Nihewan.** A, 3-D reconstruction of the pathologic tibia; B1-B2, anteroposterior
674   longitudinal sections; C1-C2, mediolateral longitudinal sections; D1-D8, cross sections; D1-D5,
675   the upper part of the tibia; D6, the upper and middle parts of the fracture; D7, the middle and
676   lower parts of the fracture; D8, lower part of the fracture, infection with subtle cortical loss.
677   MC1-MC3, represent the medullar cavities of the three fractions of the fractured tibia; NP,
678   nutrient foramen.

679   **Figure 5 Lower molars from SSMZ as compared to living hypercarnivorous taxa.** Occlusal
680   views of lower molars, m1-3, of *Canis chihliensis* (A-C) from SSMZ in Nihewan, as compared
681   with those of *C. lupus* (D), *Cuon alpinus* (E) and *Lycaon pictus* (F). A, right m1-3 (IVPP
682   V17755.6); B, right m1-3 (IVPP V17755.4); C, left (inverted) m1-2 (IVPP V17755.5); D, right
683   m1-3 (IOZ no number, extant, China); E, right m1-2 (IOZ 26747, extant, China); F, right m1-3
684   (T.M. No. 5560 and BPI/C 223, extant, South Africa). Modified from Tong et al. (2012)
685

Dimensional comparisons between the normal and pathologic tibiae of *C. chihliensis* (in: mm).

Abbreviations: DAP: anteroposterior diameter; DT: transverse diameter.

2 Table 1 Dimensional comparisons between the normal and pathologic tibiae of *C. chihliensis* (in:

3 mm). Abbreviations: DAP: anteroposterior diameter; DT: transverse diameter.

Dimensions	Normal (left) tibia (IVPP V 18139.21)	Pathologic (right) tibia (IVPP V 18139.20)
Maximum length	181.6	166.5
Proximal DAP	37.5	>32.2
Proximal DT	36.5	35.8
Distal DAP	17.6	>17.3
Distal DT	24.1	25.7
Shaft DAP at nutrient foramen	15.4	17.2
Shaft DT at nutrient foramen	13.2	14.8
Shaft DAP at the fracture	-	25.5
Shaft DT at the fracture	-	29.2

Figure 1

Two dentaries of the same individual of *Canis chihliensis*.

A, left dentary (IVPP V17755.11); B, right dentary (IVPP V17755.12). A1, B1, occlusal views; A2, B2, buccal views; A3, B3, lingual views; A4, B4, X-ray images. White arrows mark resorption of alveolar bone; red arrows mark periodontal pocket, purple arrows indicate probable fistula from periodontal pocket, blue arrows mark periapical infections associated with exposed pulp chambers, and white arrows indicate porous cortical bone.
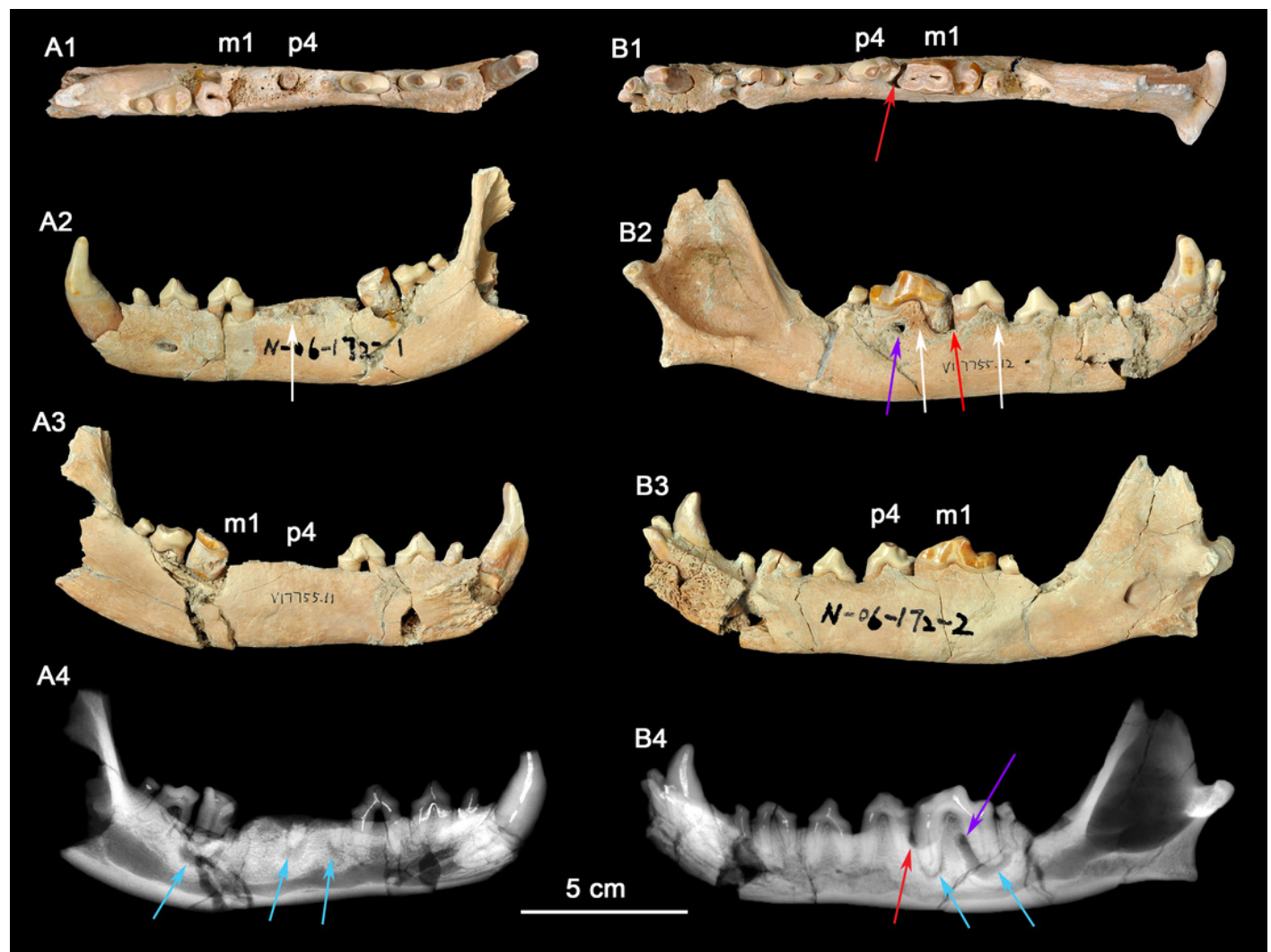
Figure 2

Frequencies of dental injury in the mandible of Rancho La Brea dire wolves, *C. dirus*.

A, numbers of specimens of adult age bearing injuries similar to those in *C. chihliensis* (orange) compared with other dental injuries (gray). Most dental injuries in *C. dirus* involve abscesses and alveolar resorption stemming from infection. B, categorization of dental injuries by tooth position. The m1 shows the highest frequency of infection or injury, followed by p2 and p4.
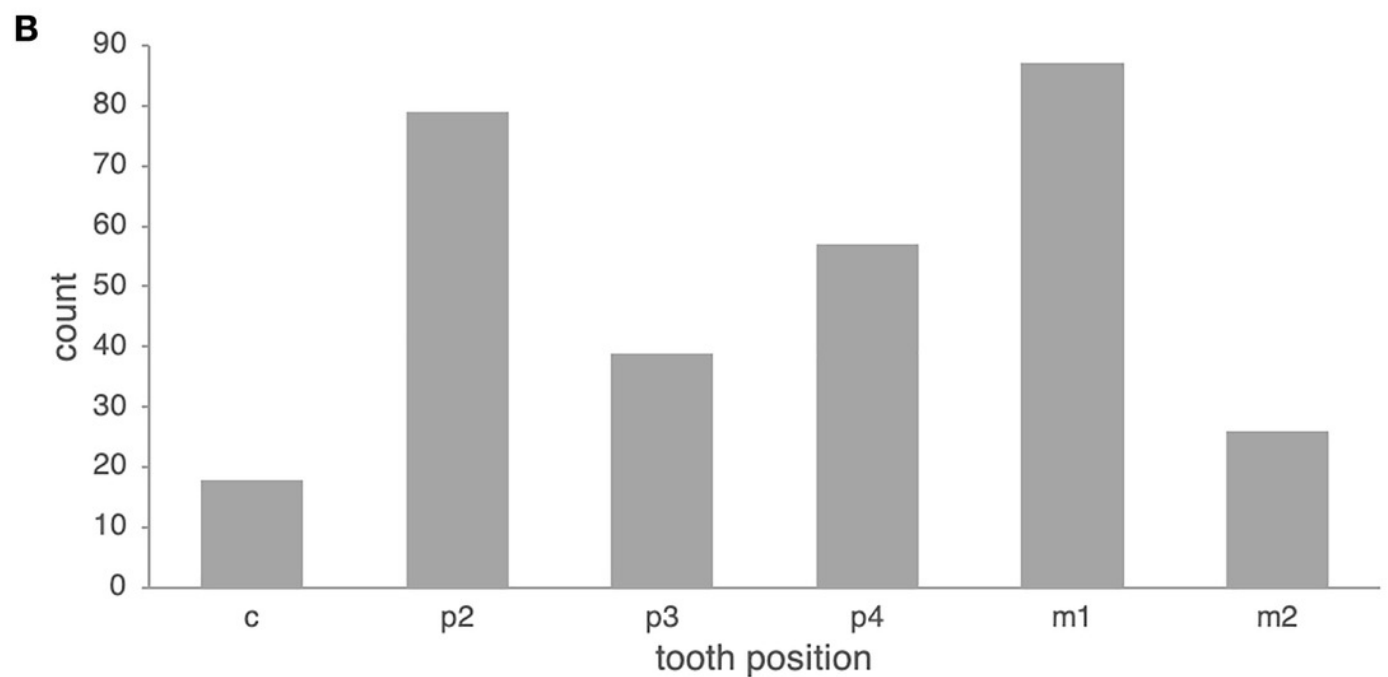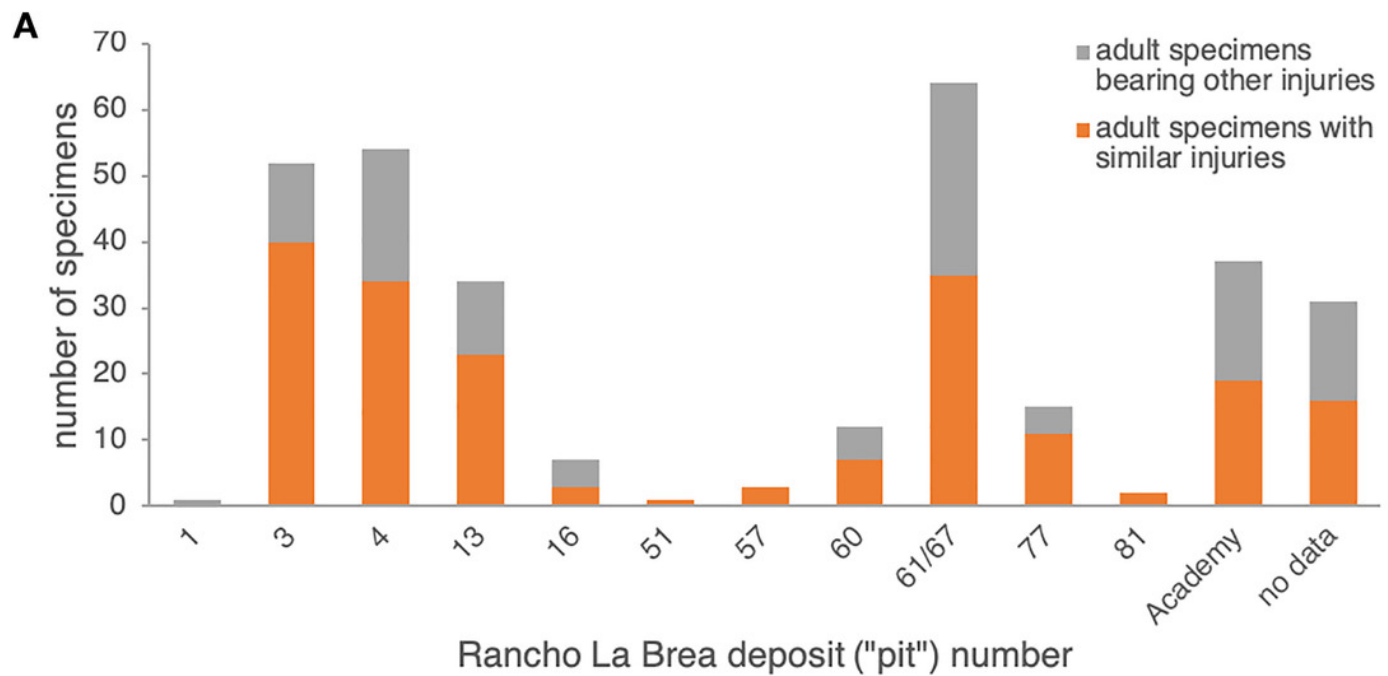
Figure 3

Tibias of the same individual of *Canis chihliensis* from SSMZ, Nihewan.

A, normal tibia of left side (IVPP V 18139.21); B, pathologic tibia of right side (IVPP V 18139.20); A1, B1, anterior views; A2, B2, posterior views; A3, B3, medial views; A4, B4, lateral views. NF: nutrient foramen.

Figure 4

CT scan images of the pathologic right tibia of *Canis chihliensis* (V18139-20) from SSMZ, Nihewan.

A, 3-D reconstruction of the pathologic tibia; B1-B2, anteroposterior longitudinal sections; C1-C2, mediolateral longitudinal sections; D1-D8, cross sections; D1-D5, the upper part of the tibia; D6, the upper and middle parts of the fracture; D7, the middle and lower parts of the fracture; D8, lower part of the fracture, infection with subtle cortical loss. MC1-MC3, represent the medullar cavities of the three fractions of the fractured tibia; NP, nutrient foramen.

Figure 5

Lower molars from SSMZ as compared to living hypercarnivorous taxa.

Occlusal views of lower molars, m1-3, of *Canis chihliensis* (A-C) from SSMZ in Nihewan, as compared with those of *C. lupus* (D), *Cuon alpinus* (E) and *Lycaon pictus* (F). A, right m1-3 (IVPP V17755.6); B, right m1-3 (IVPP V17755.4); C, left (inverted) m1-2 (IVPP V17755.5); D, right m1-3 (IOZ no number, extant, China); E, right m1-2 (IOZ 26747, extant, China); F, right m1-3 (T.M. No. 5560 and BPI/C 223, extant, South Africa). Modified from Tong et al. (2012)